Scaling of Dynamical Decoupling for Spin Qubits

J. Medford,[1] Ł. Cywiński,[2] C. Barthel,[1] C. M. Marcus,[1] M. P. Hanson,[3] and A. C. Gossard[3]
[1]Department of Physics, Harvard University, Cambridge, Massachusetts 02138, USA
[2]Institute of Physics, Polish Academy of Sciences, Al. Lotników 32/46, PL 02-668 Warszawa, Poland
[3]Materials Department, University of California, Santa Barbara, California 93106, USA
(Received 18 August 2011; published 23 February 2012)

We investigate the scaling of coherence time T_2 with the number of π pulses n_π in a singlet-triplet spin qubit using Carr-Purcell-Meiboom-Gill (CPMG) and concatenated dynamical decoupling (CDD) pulse sequences. For an even numbers of CPMG pulses, we find a power law $T_2 \propto (n_\pi)^{\gamma_e}$, with $\gamma_e = 0.72 \pm 0.01$, essentially independent of the envelope function used to extract T_2. From this surprisingly robust value, a power-law model of the noise spectrum of the environment, $S(\omega) \sim \omega^{-\beta}$, yields $\beta = \gamma_e/(1-\gamma_e) = 2.6 \pm 0.1$. Model values for $T_2(n_\pi)$ using $\beta = 2.6$ for CPMG with both even and odd n_π up to 32 and CDD orders 3 through 6 compare very well with the experiment.

DOI: 10.1103/PhysRevLett.108.086802 PACS numbers: 85.35.Be, 03.67.Ac

A variety of solid state systems are emerging as effective platforms for studying decoherence and entanglement in controlled quantum systems [1–4]. Among them, quantum-dot-based spin qubits have recently achieved sufficient control and long coherence times [1,2] that new information about the noise environment of the qubit can be extracted, complementing related work in nitrogen-vacancy centers in diamond [4], superconducting qubits [3], trapped ions [5], and neutral atoms [6].

Dynamical decoupling in the form of a sequence of π pulses [7–10] functions as a high-pass filter, thus providing information about the spectral content of environmental noise [3–5,11–16]. For spin qubits, the effectiveness of various decoupling schemes at mitigating dephasing due to nuclear bath dynamics has been well-studied theoretically [17–21]. Much less is known about mitigating the effects of charge noise, which couples to the qubit via gate-dependent exchange interaction and through spatially varying Overhauser fields [1]. When the decoherence time T_2 is short compared to the energy relaxation time T_1—which is the case in this study—both the envelope of the coherence decay as well as the dependence of T_2 on the number of π pulses, n_π, depend on the spectral density of the environment, $S(\omega)$. Knowledge of $S(\omega)$ inferred from such measurements can in turn be used to design optimal decoupling sequences [5,12,22–24].

In this Letter, we investigate the scaling of T_2 with the number of π pulses for Carr-Purcell-Meiboom-Gill (CPMG) and concatenated dynamical decoupling (CDD) sequences in a GaAs two-electron singlet-triple qubit [Fig. 1(a)]. The coherence envelope is reasonably well-described by the form $\exp[-(\tau_D/T_2)^\alpha]$, where τ_D is the time during which π pulses are applied [Fig. 2(b)]. It is difficult, however, to accurately determine α by directly fitting to this form. In contrast, we find that the scaling relation $T_2 \sim (n_\pi)^\gamma$ very accurately describes the data, irrespective of the value of α used to extract T_2. The resulting γ can then be related to α and other quantities of interest within specific noise models. For CPMG with even n_π, the scaling relation $T_2 \propto (n_\pi)^{\gamma_e}$ yields $\gamma_e = 0.72 \pm 0.01$, using T_2 values extracted using any α in the range of 2 to 5. A model of dephasing due to a power-law spectrum of classical noise, $S(\omega) \sim \omega^{-\beta}$, leads to a scaling relation in the number of π pulses, with the exponent of the power law β related to the scaling exponent by the simple relation $\beta = \gamma_e/(1-\gamma_e)$. For the present experiment, $\gamma_e = 0.72$ thus yields $\beta = 2.6$. Further support for a power-law form for $S(\omega)$ is found by comparing experimental and theoretical dependences $T_2(n_\pi)$ for CPMG with both even and odd n_π as well as CDD pulse sequences. This model also gives the simple relation $\alpha = \beta + 1$, connecting the noise spectrum and the decoherence envelope exponent. The resulting value, $\alpha = 3.6 \pm 0.1$, is thus determined with considerably greater accuracy than can be obtained from direct fits to the coherence envelope data.

The lateral double quantum dot investigated was defined by Ti/Au depletion gates patterned using electron beam

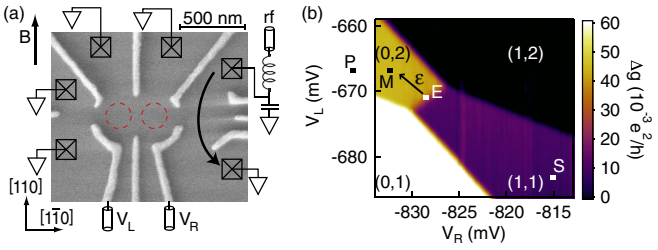

FIG. 1 (color online). (a) Micrograph of a lithographically identical device with dot locations depicted. The gate voltages $V_{R(L)}$ set the charge occupancy of the right (left) dot as well as the detuning of the qubit. An rf-sensor quantum dot is indicated on the right. (b) Double-dot charge state mapped onto dc conductance change, Δg, with lettered pulse sequence gate voltages. The detuning axis is orthogonal to the (0,2)–(1,1) charge degeneracy through points E, S, and M.

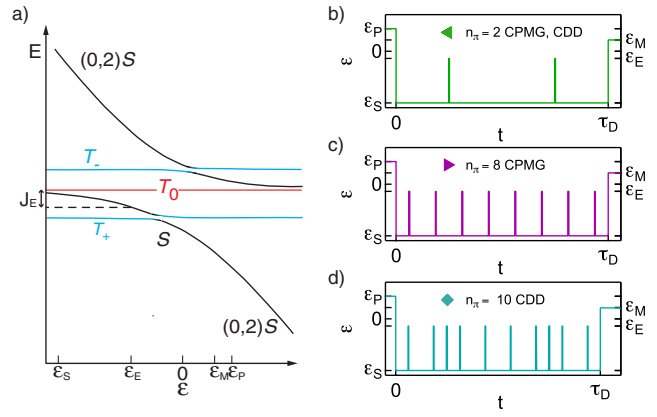

FIG. 2 (color online). (a) Energy level diagram along the detuning axis ϵ. The (0,2) singlet was prepared at ϵ_P, followed by separation to ϵ_S. π pulses are performed at ϵ_E, allowing for subsequent rephasing at ϵ_S. There is a single-shot readout at ϵ_M using a proximal sensor dot. The exchange energy J_E that drives the π pulses at ϵ_E is indicated with a dashed line. (b)–(d) Schematics of detunings during CPMG and CDD pulse sequences with detuning points on the vertical axis.

lithography on a $GaAs/Al_{0.3}Ga_{0.7}As$ heterostructure with a two-dimensional electron gas (density 2×10^{15} m^{-2}, mobility 20 m^2/V s) 100 nm below the surface. Measurements were performed in a dilution refrigerator with an electron temperature $T_e \sim 150$ mK. The double quantum dot is operated as a spin qubit by first depleting the quantum dots to the last two electrons and then manipulating the charge occupancy of the two dots with high-bandwidth plunger gates V_L and V_R along a detuning axis ϵ [Fig. 1(b)]. In this work, the charge occupancy was manipulated between states (0,2) and (1,1), where N_L and N_R represent the charge in the left and right dots. Charge occupancy was determined by the conductance change Δg through a proximal sensor quantum dot, which in turn modulated the reflection coefficient of the radio-frequency (rf) readout circuit [25,26].

The logical spin qubit subspace is spanned by the singlet $[S = (|\uparrow\downarrow\rangle - |\downarrow\uparrow\rangle)/\sqrt{2}]$ and the $m = 0$ triplet $[T_0 = (|\uparrow\downarrow\rangle + |\downarrow\uparrow\rangle)/\sqrt{2}]$ states of two electrons. The $m = \pm 1$ triplet states were split off by a 750 mT magnetic field applied in the plane of the electron gas, perpendicular to the dot connection axis. A (0,2) singlet was prepared at point P, off the detuning axis, through rapid relaxation to the ground state, then moved to the separation point S in (1,1). Uncorrelated Overhauser fields in the two dots create an evolving Zeeman gradient ΔB_z that drives transitions between S and T_0. A single-shot readout was performed by moving to point M, where S can tunnel to (0,2) while T_0 remains in (1,1). The reflectometer signal was integrated for 600 ns per shot, averaged over 10^4 shots, and compared to voltage values corresponding to S and T_0 outcomes [27], yielding $P_S(\tau_D)$, the probability of singlet return.

Coherence lost due to the (thermally driven) evolution of ΔB_z can be partially restored using a Hahn echo by pulsing at time $\tau_D/2$ to point E, where the exchange splitting between S and T_0 drives a π rotation about the $\hat{x}$ axis, changing the sign of the acquired phase. Returning to S for an equal time $\tau_D/2$ cancels the phase acquired due to the low-frequency ($\omega < 2/\tau_D$) end of the spectrum of fluctuations of ΔB_z [11,12]. Dynamical decoupling using a series of π pulses allows efficient removal of more of the low-frequency end of the noise spectrum [11,12]. The CPMG sequence [28], for example, uses evenly spaced gate pulses from point S to point E with a half interval before the first and after the last π pulse [Figs. 2(b) and 2(c)]. CDD [2,9,29] uses nonuniformly spaced pulses to point E, where the kth-order sequence is determined recursively from the lower-order one, with an additional π pulse in the center of odd orders (the first order of CDD corresponds here to the Hahn echo) [Fig. 2(d)].

Singlet return probabilities $P_S(\tau_D)$ were measured for CPMG sequences with $n_\pi = 1, 2, 3, 4, 8, 16$, and 32. Fits to $P_S = 0.5 + V/2 \exp[-(\tau_D/T_2)^\alpha]$, with visibility V and T_2 as fit parameters, were equally good for fixed values of α between 2 and 4, as seen in Fig. 3(a). For this reason, although $S(\omega)$ is related to α, these fits give little information about the spectrum of the environment. Figure 3(b), showing the fitted value of T_2 as a function of the fixed α and n_π for an even number of CPMG pulses, shows two remarkable features. First, values of T_2 do not depend on the value of α used in the fits to $P_S(\tau_D)$. Second, T_2 shows a power-law scaling $T_2 = T_2^0(n_\pi)^\gamma$ whose power, γ, also does not depend on the value of α used in the fits.

To model these observations, we consider the Gaussian noise affecting the energy splitting of the qubit, which leads to the off-diagonal (in the basis of $|\uparrow\downarrow\rangle$ and $|\downarrow\uparrow\rangle$) elements of the qubit density matrix decaying as $\exp[-\chi(\tau_D)]$, where

$$\chi(\tau_D) = \int_0^\infty \frac{d\omega}{\pi} S(\omega) \frac{F(\omega\tau_D)}{\omega^2}, \tag{1}$$

with $F(\omega\tau_D)$ being the filter function determined by the sequence of π pulses driving the qubit. For the CPMG sequence, $F(z) < (z/2n_\pi)^4$ for $z < 2n_\pi$, i.e., $F(z)$ strongly suppresses the low-frequency noise, while, for large z and n_π, the filter function can be approximated [12] by a periodic train (with period $z_p = 2\pi n_\pi$) of square peaks of height $h \approx 2n_\pi^2$ and width $\Delta z \approx z_p^2/\pi h \ll z_p$.

We find that the value of γ_e and the presence of an even-odd effect (EOE) in n_π (i.e., $\gamma_e \neq \gamma_o$) act as discriminators for several classes of $S(\omega)$. (i) The case of $0 < \gamma_e \leq 2/3$ and absent EOE is compatible with a model of $S(\omega) \sim \omega^{-\beta}$ (over a range of ω roughly bounded by the minimal and maximal values of n_π/τ_D), with $0 < \beta \leq 2$. In this case, $\gamma_e = \beta/(1+\beta)$ and $\alpha = \beta + 1$. This can be derived by realizing that the contribution to $\chi(\tau_D)$ for CPMG is dominated by a narrow peak of height $2n_\pi^2$ at $\omega\tau_D \approx \pi n_\pi$ in the $F(\omega\tau_D)$ filter [3,12,15,16]. One example is the

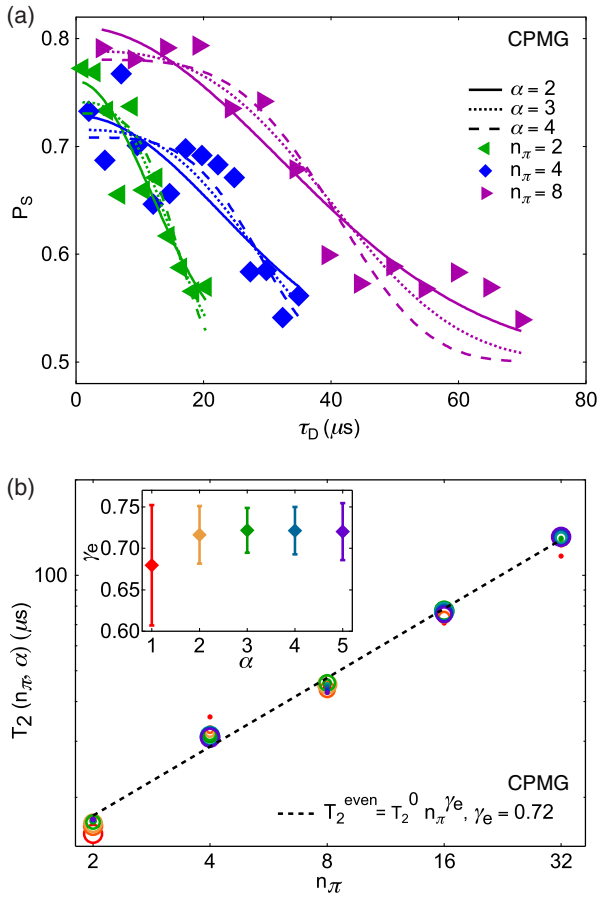

FIG. 3 (color online). (a) Experimental singlet return probabilities as a function of time for CPMG with $n_\pi = 2, 4, 8$. Fits to $P_S(\tau_D) = 0.5 + V/2 \exp[-(\tau_D/T_2)^\alpha]$, with α constrained to 2 (solid curves), 3 (dotted curves), and 4 (dashed curves) [34]. It is difficult to determine α from these fits. (b) Extracted T_2 for even-n_π CPMG sequences for α constrained to 1, 2, 3, 4, and 5. The circle size is proportional to the χ^2 goodness of fit of $P_S(\tau_D)$ in (a). A power-law fit to the form $\ln[T_2^{\text{even}}(\alpha)] = \ln(T_2^0) + \gamma_e \ln(n_\pi)$, shown for $\alpha = 3$ (dashed line), gives $\gamma_e = 0.72$. The fit value γ_e depends only weakly on α in the range 2–5 (inset). The weighted average over $\alpha = 2$–5 yields $\gamma_e = 0.72 \pm 0.01$.

case of Ornstein-Uhlenbeck noise [30] [having Lorentzian $S(\omega)$, with the ω^{-2} tail typically dominating the decoherence under dynamical decoupling], where $\gamma = 2/3$ was confirmed by experiments on the NV center [4]. (ii) When an EOE is present, $\gamma_e = 2/3$ suggests a hard cutoff in $S(\omega)$ at $\omega_c < 2/T_2$, in which case $\gamma_o = 1$. (iii) For $\omega_c > 2/T_2$, i.e., for larger ω_c or larger n_π (leading to longer T_2), the EOE disappears and γ tends to 1 [14]. (iv) Finally, the presence of the EOE and $2/3 < \gamma_e < 1$ indicates $S(\omega) \sim \omega^{-\beta}$, with $\beta > 2$.

Experimentally, we find $\gamma_e = 0.72$ for an even number of CPMG pulses, and $n_\pi = 1$ not along the scaling line, indicating an EOE. We conclude that scenario (iv) applies, namely, $S(\omega) = A^{\beta+1}/\omega^\beta$ with $2 < \beta < 3$. Using Eq. (1) and the CPMG filter function gives, in the large-n_π limit,

$$\chi(t) \approx (A\tau_D)^{1+\beta}\left(\frac{a}{n_\pi^\beta} + \frac{b_{e/o}}{n_\pi^4}\right), \tag{2}$$

with $a \approx \Sigma_{2+\beta}/\pi^2(2\pi)^\beta$, where $\Sigma_\delta = \sum_{k=1}^\infty (k - \frac{1}{2})^{-\delta}$, and, for odd (even) n_π, we have $b_o \approx [32\pi(3-\beta)]^{-1}$ $\{b_e \approx [128\pi(5-\beta)]^{-1} \approx b_o/10\}$; i.e., the b/n_π^4 term is negligible for even n_π, while it gives a significant correction for small, odd n_π. The EOE comes from the difference in the low-z behavior of the CPMG filter functions, which, for $z < 1$, behave as $F(z) \sim z^4/2^5 n_\pi^4 (z^6/2^7 n_\pi^4)$ for odd (even) n_π. For $\beta > 2$, this leads to different contributions of very low ω to the integral in Eq. (1). For even n_π, we find that $\chi(\tau_D)$ approximately reduces to $(A\tau_D)^{1+\beta} a/n_\pi^\beta$, from which we obtain the $\beta \leq 2$ result of $\gamma_e = \beta/(1+\beta)$ in this case, as well. Note that, in Fig. 3(b), we fit a parameter $T_2^0 = [Aa^{1/(1+\beta)}]^{-1}$, which corresponds to a hypothetical echo decay time in the absence of very low-ω noise [i.e., putting $F(z) = 0$ for $z < 1$].

Assuming this form of $S(\omega)$, fits to the even n_π [Fig. 3(b)] yield $\beta = 2.6$ and $A^{-1} = 3.6$ μs. Using these two parameters, we calculate odd-n_π values for T_2 by numerically integrating Eq. (1). As shown in Fig. 4, the obtained value of T_2 is in good agreement with the measured value for $n_\pi = 1$ (Hahn echo). We note that the large n_π scaling of $T_2 \sim n_\pi^\gamma$ is due to the behavior of $S(\omega)$ at $\omega \geq \pi n_\pi/T_2$, which is $\sim 0.3(n_\pi)^{0.28}$ μs^{-1} here, while the EOE at small n_π is due to behavior at $\omega < 1/T_2$, which is ~ 0.15 μs^{-1}. The consistency between small- and large-n_π data indicates that $S(\omega) \sim \omega^{-2.6}$ over this range of frequencies (i.e., $\omega/2\pi \sim 10$–100 kHz). The EOE behavior at low n_π can be fit within scenario (ii) using $S(\omega) = A^3\omega^2$ with $A^{-1} \sim 1$ μs and $\omega_c \sim 0.08$ μs^{-1}. However, this scenario crosses over to (iii) for $n_\pi > 5$, where γ tends to 1. The resulting large-n_π behavior, $T_2 \sim n_\pi \times 7$ μs, departs significantly from the $n_\pi \geq 8$ data in Fig. 4.

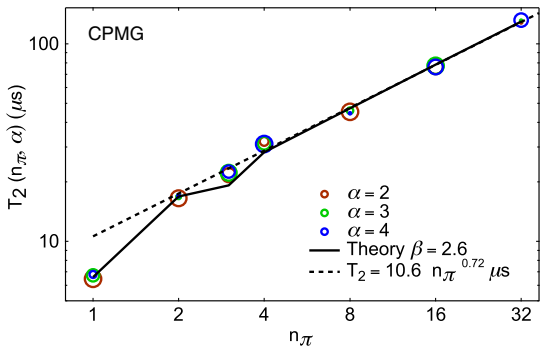

FIG. 4 (color online). T_2 for all measured n_π for CPMG, extracted using $\alpha = 2$, 3, and 4 (circles). The circle size for each α is proportional to the χ^2 goodness of fit. Theory (black solid curve) for the integration of Eq. (1) with the CPMG filter functions and $\beta = \gamma_e/(1-\gamma_e) = 2.6$. Note that Eq. (2) captures the even/odd effect quantitatively for small n_π. The black dashed line is the power-law fit to the even n_π points.

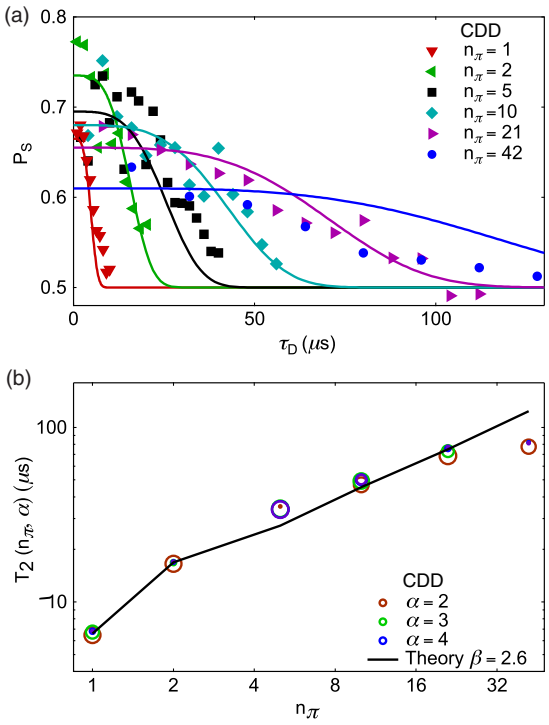

FIG. 5 (color online). (a) Experimental singlet return probabilities for orders 1 through 6 CDD (symbols), along with fits to $P_S(\tau_D) = 0.5 + V/2 \exp[-(\tau_D/T_2)^\alpha]$ using $\beta = \gamma_e/(1-\gamma_e) = 2.6$ (solid curves). (b) Extracted T_2 for using different values of α (the circle size is proportional to the χ^2 measure of goodness of fit). The theory (solid curve) is based on $\beta = \gamma_e/(1-\gamma_e) = 2.6$ and the integration of Eq. (1) with the appropriate CDD filter function [12].

Using $S(\omega) = A^{\beta+1}/\omega^\beta$ with parameters A and β fixed from the even-n_π CPMG fit, we can calculate the expected dependence of $T_2(n_\pi)$ for the CDD pulse sequence using the known filter functions [12]. For $n_\pi = 5$, 10, and 21, we get good agreement between the calculated and measured T_2 [Fig. 5]. For $n_\pi = 42$, the experimental T_2 is shorter than predicted by theory, possibly reflecting an accumulation of errors for such a large number of pulses. Note that CDD was shown to be robust to pulse errors [31] only in the case of two-axis control (i.e., when the π pulses are about x and y axes alternately) and for a quasistatic bath.

Let us note that $S(\omega)$ of a very similar form ($\sim 1/\omega^{2.5}$) was recently inferred in Ref. [32] from the transport data taken from Ref. [33]. The strong low-frequency noise was tentatively ascribed to electron current shot noise, generating much slower Overhauser field dynamics.

Summarizing, the measurements of qubit decoherence under dynamical decoupling with the CPMG pulse sequence have been used to reconstruct the crucial features of the spectral density of noise dephasing the qubit. Using the data for even n_π of CPMG, we have been able to estimate the magnitude of noise and its functional form. The reconstructed spectral density of noise allows us to calculate the expected decoherence signal for other pulse sequences, and this calculation agrees with the CDD sequence measurements for n_π as well as the odd-n_π CPMG data. We have shown that, instead of fitting the exact functional form of the coherence decay function, an analysis of the scaling of the measured T_2 time with the number of applied pulses allows for a clearer understanding of the system. We cannot say at this point whether the observed value $\gamma_e = 0.72$ is characteristic of Overhauser-dominated dephasing in general or just our particular combination of noise sources.

We acknowledge funding from IARPA under the MQCO program, from NSF under the Materials World Network program, and from the Homing Programme of the Foundation for Polish Science supported by the EEA Financial Mechanism (Ł. C.). We thank M. Biercuk and V. Dobrovitski for useful discussions.

[1] H. Bluhm, S. Foletti, I. Neder, M. Rudner, D. Mahalu, V. Umansky, and A. Yacoby, Nature Phys. **7**, 109 (2011).
[2] C. Barthel, J. Medford, C. M. Marcus, M. P. Hanson, and A. C. Gossard, Phys. Rev. Lett. **105**, 266808 (2010).
[3] J. Bylander, S. Gustavsson, F. Yan, F. Yoshihara, K. Harrabi, G. Fitch, D. G. Cory, Y. Nakamura, J.-S. Tsai, and W. D. Oliver, Nature Phys. **7**, 565 (2011).
[4] G. de Lange, Z. H. Wang, D. Ristè, V. V. Dobrovitski, and R. Hanson, Science **330**, 60 (2010).
[5] M. J. Biercuk, H. Uys, A. P. VanDevender, N. Shiga, W. M. Itano, and J. J. Bollinger, Nature (London) **458**, 996 (2009).
[6] Y. Sagi, I. Almog, and N. Davidson, Phys. Rev. Lett. **105**, 053201 (2010).
[7] L. Viola and S. Lloyd, Phys. Rev. A **58**, 2733 (1998).
[8] G. S. Uhrig, Phys. Rev. Lett. **98**, 100504 (2007).
[9] K. Khodjasteh and D. A. Lidar, Phys. Rev. A **75**, 062310 (2007).
[10] K. Khodjasteh, T. Erdélyi, and L. Viola, Phys. Rev. A **83**, 020305 (2011).
[11] R. de Sousa, Top. Appl. Phys. **115**, 183 (2009).
[12] Ł. Cywiński, R. M. Lutchyn, C. P. Nave, and S. Das Sarma, Phys. Rev. B **77**, 174509 (2008).
[13] M. J. Biercuk, A. C. Doherty, and H. Uys, J. Phys. B **44**, 154002 (2011).
[14] M. J. Biercuk and H. Bluhm, Phys. Rev. B **83**, 235316 (2011).
[15] G. A. Alvarez and D. Suter, Phys. Rev. Lett. **107**, 230501 (2011).
[16] T. Yuge, S. Sasaki, and Y. Hirayama, Phys. Rev. Lett. **107**, 170504 (2011).
[17] W. Yao, R.-B. Liu, and L. J. Sham, Phys. Rev. B **74**, 195301 (2006).
[18] W. M. Witzel and S. Das Sarma, Phys. Rev. B **74**, 035322 (2006).
[19] W. M. Witzel and S. Das Sarma, Phys. Rev. Lett. **98**, 077601 (2007).
[20] Ł. Cywiński, W. M. Witzel, and S. Das Sarma, Phys. Rev. B **79**, 245314 (2009).

[21] I. Neder, M. S. Rudner, H. Bluhm, S. Foletti, B. I. Halperin, and A. Yacoby, Phys. Rev. B **84**, 035441 (2011).
[22] G. Gordon, G. Kurizki, and D. A. Lidar, Phys. Rev. Lett. **101**, 010403 (2008).
[23] Y. Pan, Z.-R. Xi, and W. Cui, Phys. Rev. A **81**, 022309 (2010).
[24] A. Ajoy, G. A. Álvarez, and D. Suter, Phys. Rev. A **83**, 032303 (2011).
[25] D. J. Reilly, C. M. Marcus, M. P. Hanson, and A. C. Gossard, Appl. Phys. Lett. **91**, 162101 (2007).
[26] C. Barthel, M. Kjærgaard, J. Medford, M. Stopa, C. M. Marcus, M. P. Hanson, and A. C. Gossard, Phys. Rev. B **81**, 161308(R) (2010).
[27] C. Barthel, D. J. Reilly, C. M. Marcus, M. P. Hanson, and A. C. Gossard, Phys. Rev. Lett. **103**, 160503 (2009).
[28] L. M. K. Vandersypen and I. L. Chuang, Rev. Mod. Phys. **76**, 1037 (2005).
[29] X. Peng, D. Suter, and D. A. Lidar, J. Phys. B **44**, 154003 (2011).
[30] V. V. Dobrovitski, A. E. Feiguin, R. Hanson, and D. D. Awschalom, Phys. Rev. Lett. **102**, 237601 (2009).
[31] Z.-H. Wang, W. Zhang, A. M. Tyryshkin, S. A. Lyon, J. W. Ager, E. E. Haller, and V. V. Dobrovitski, arXiv:1011.6417.
[32] M. S. Rudner, F. H. L. Koppens, J. A. Folk, L. M. K. Vandersypen, and L. S. Levitov, Phys. Rev. B **84**, 075339 (2011).
[33] F. H. L. Koppens, J. A. Folk, J. M. Elzerman, R. Hanson, L. H. W. van Beveren, I. T. Vink, H. P. Tranitz, W. Wegscheider, L. P. Kouwenhoven, and L. M. K. Vandersypen, Science **309**, 1346 (2005).
[34] CPMG visibilities for $\alpha = 2$ are $n_\pi = 2, V = 0.52 \pm 0.02$; $n_\pi = 4$, $V = 0.46 \pm 0.04$; and $n_\pi = 8$, $V = 0.62 \pm 0.02$. Visibilities for $\alpha = 3$ are $n_\pi = 2$, $V = 0.48 \pm 0.03$; $n_\pi = 4$, $V = 0.43 \pm 0.02$; and $n_\pi = 8$, $V = 0.58 \pm 0.03$. Visibilities for $\alpha = 4$ are $n_\pi = 2$, $V = 0.46 \pm 0.03$; $n_\pi = 4$, $V = 0.42 \pm 0.02$; and $n_\pi = 8$, $V = 0.56 \pm 0.03$.